Journal of Sound and Vibration 329 (2010) 4294–4312

Contents lists available at ScienceDirect

Journal of Sound and Vibration

journal homepage: www.elsevier.com/locate/jsvi

Modal identification based on Gaussian continuous time autoregressive moving average model

Du Xiuli [a,*], Wang Fengquan [b]

[a] School of Mathematical Sciences, Nanjing Normal University, 210046, PR China
[b] College of Civil Engineering, Southeast University, 210096, PR China

ARTICLE INFO

Article history:
Received 7 February 2009
Received in revised form
11 April 2010
Accepted 17 April 2010
Handling Editor: L.G. Tham
Available online 11 May 2010

ABSTRACT

A new time-domain modal identification method of the linear time-invariant system driven by the non-stationary Gaussian random force is presented in this paper. The proposed technique is based on the multivariate continuous time autoregressive moving average (CARMA) model. This method can identify physical parameters of a system from the response-only data. To do this, we first transform the structural dynamic equation into the CARMA model, and subsequently rewrite it in the state-space form. Second, we present the exact maximum likelihood estimators of parameters of the continuous time autoregressive (CAR) model by virtue of the Girsanov theorem, under the assumption that the uniformly modulated function is approximately equal to a constant matrix over a very short period of time. Then, based on the relation between the CAR model and the CARMA model, we present the exact maximum likelihood estimators of parameters of the CARMA model. Finally, the modal parameters are identified by the eigenvalue analysis method. Numerical results show that the method we introduced here not only has high precision and robustness, but also has very high computing efficiency. Therefore, it is suitable for real-time modal identification.

1. Introduction

In the field of engineering structures, identifying structural modal parameters or physical parameters means extracting the structural information from both the structural excitation and the response data or only from the response data. However, the random excitation in an ambient vibration test, which acts on bridges and large buildings, is usually too complicated to be known or measured, so one has to determine the modal parameters from the response data.

In the last several decades, a series of mature methods have been presented for modal identification subject to the stationary ambient excitation, but that is not the case for non-stationary situations. Up to now, the better and widely applied methods for non-stationary situations focus mainly on the time domain and the time–frequency analysis domain. These methods have their merits in extracting modal parameters from the measured data. In this paper, we discuss mainly the modal identification methods in time domain. The mature time-domain methods are mainly based upon the time series models and the structural inversion algorithm.

As a powerful technique for analyzing non-stationary signals, the autoregressive integrated moving average (ARIMA) model has been widely used in a variety of engineering subjects. To use this method, at first we need to carry out the difference operation with the non-stationary time series till the resulting series is stationary and thus constant ARMA

* Corresponding author.
E-mail address: seuam@sina.com.cn (X.L. Du).

0022-460X/$ - see front matter © 2010 Elsevier Ltd. All rights reserved.
doi:10.1016/j.jsv.2010.04.018

model coefficients are obtained by the model identification. However, the corresponding relationship of parameters between the structural dynamic model and the ARMA model is quite complicated, especially for the MDOF system.

In Refs. [1–3], Li, Chen and Joo et al. discussed the structural inversion algorithm of the LTI system subject to the ambient excitation. The method can estimate both system parameters and inputs by the recursive algorithm. Nevertheless, the method is computationally intensive due to its iterative nature, and it is unpractical for applications.

Because the response of the system subject to the non-stationary excitation is non-stationary too, it is appropriate to study it with both the ARMA model with non-stationary stochastic error and the continuous time-varying ARMA model (TARMA). Sakellariou and Fassois discussed the ARMA model with non-stationary stochastic error in Ref. [4]. Liu [5] built the link between the continuous time-varying ARMA model and the discrete time-varying ARMA model. Poulimenos and Fassois [6] gave an overall view of methods on identifying parameters of the discrete time-varying ARMA model. Based on it, Jachan et al. [7] presented a new time–frequency ARMA model for non-stationary signals. The TARMA model differs from their conventional, stationary, counterparts in that their parameters are time-dependent. Methods based upon them are known to offer a number of potential advantages, such as representation parsimony; improved accuracy; improved resolution; improved tracking of the time-varying dynamics; flexibility in analysis; capturing directly the underlying structural dynamics responsible for the non-stationary behavior. Inevitably, these methods suffer also from, such as, the complication of the corresponding relationship between the continuous and discrete ARMA models and the iterative nature in computation.

Besides, some researchers presented some time-domain modal identification methods from different aspects. Toolan [8] presented a random subspace method for the system subject to the non-stationary excitation. Mohanty [9] improved the Ibrahim method when the system is driven by the harmonic excitation.

This paper presents a new efficient time-domain identification procedure to identify the physical parameters and the dynamic characteristics of a structural system, namely, the stiffness, damping, natural frequencies, modal damping ratios, and modal shapes, by using the continuous time autoregressive moving average model under the non-stationary ambient excitation. These models will be introduced in Section 2, we also give a brief exposition of their state space forms. Section 3 transforms the structural dynamic equation of the system into the continuous time autoregressive moving average model. Section 4, which provides the main contributions of this paper, presents the estimator of the uniformly modulated function and the exact maximum likelihood estimators of parameters. Section 5 demonstrates the applicability of the method by numerical simulations. Some conclusions are presented in Section 6.

2. Multivariate Gaussian CARMA process

Definition 2.1. An n-dimensional continuous-time Gaussian autoregressive moving average (CARMA) process (for more details, see [10]) of order p,q $(0 \le q < p)$ is defined symbolically to be a solution of the stochastic differential equation

$$\mathbf{A}(D)\mathbf{X}(t) = \mathbf{J}(t) + \boldsymbol{\sigma}_0(t)D\mathbf{W}(t) + \cdots + \boldsymbol{\sigma}_q(t)D^{q+1}\mathbf{W}(t), \tag{1}$$

where $\mathbf{A}(D) = \mathbf{I}_n D^p + \mathbf{A}_1 D^{p-1} + \cdots + \mathbf{A}_p$, $\mathbf{A}_i$ $(i = 1, \ldots, p)$ is the $n \times n$ matrix, $\mathbf{I}_n$ is an n-dimensional identity matrix, the operator D denotes differentiation with respect to t; $\mathbf{J}(t)$ and $\boldsymbol{\sigma}_i(t)$ $(i=0,\ldots,q)$ are the n-dimensional column vector and the $n \times n$ non-singular matrix, respectively. $\boldsymbol{\sigma}_i(t)$ is called the uniformly modulated function, $\boldsymbol{\sigma}_i(t) = \mathbf{0}$ $(i=q+1,\ldots,p)$. $\{\mathbf{W}_t, \mathcal{F}_t; 0 \le t < \infty\}$ is an n-dimensional Brownian motion. Since $D^i\mathbf{W}(t)$ $(i = 1, \ldots, q+1)$ does not exist, we give meaning to Eq. (1) by rewriting it as the observation and state equations:

$$\mathbf{X}(t) = (\mathbf{I}_n, \mathbf{0}, \ldots, \mathbf{0})\mathbf{Y}(t) + \boldsymbol{\beta}_0(t)\,\mathrm{d}\mathbf{W}(t), \tag{2}$$

$$\mathrm{d}\mathbf{Y}(t) = \mathbf{A}\mathbf{Y}(t)\,\mathrm{d}t + \mathbf{J}(t)\,\mathrm{d}t + \mathbf{C}(t)\,\mathrm{d}\mathbf{W}(t), \tag{3}$$

where $\mathbf{Y}(t) = (\mathbf{Y}_0^{\mathrm{T}}(t), \ldots, \mathbf{Y}_{p-1}^{\mathrm{T}}(t))^{\mathrm{T}}$ denotes an np-dimensional column vector, $\mathbf{Y}_i(t)$ $(i=0,\ldots,p-1)$ is an n-dimensional column vector, superscript T denotes transposition, $\boldsymbol{\beta}_0(t) = \boldsymbol{\sigma}_p(t)$,

$$\mathbf{A} = \begin{pmatrix} \mathbf{0} & \mathbf{I}_n & \mathbf{0} & \cdots & \mathbf{0} \\ \mathbf{0} & \mathbf{0} & \mathbf{I}_n & \cdots & \mathbf{0} \\ \vdots & \vdots & \vdots & \cdots & \vdots \\ \mathbf{0} & \mathbf{0} & \mathbf{0} & \cdots & \mathbf{I}_n \\ -\mathbf{A}_p & -\mathbf{A}_{p-1} & -\mathbf{A}_{p-2} & \cdots & -\mathbf{A}_1 \end{pmatrix},$$

and $\mathbf{C}(t) = (\boldsymbol{\beta}_1^{\mathrm{T}}(t), \ldots, \boldsymbol{\beta}_p^{\mathrm{T}}(t))^{\mathrm{T}}$, where

$$\boldsymbol{\beta}_1(t) = \boldsymbol{\sigma}_{p-1}(t) - \mathbf{A}_1\boldsymbol{\beta}_0(t),$$

$$\boldsymbol{\beta}_2(t) = \boldsymbol{\sigma}_{p-2}(t) - \mathbf{A}_2\boldsymbol{\beta}_0(t) - \mathbf{A}_1\boldsymbol{\beta}_1(t) + f_2\left(\frac{\mathrm{d}\boldsymbol{\beta}_1(t)}{\mathrm{d}t}\right),$$

$$\boldsymbol{\beta}_3(t)=\boldsymbol{\sigma}_{p-3(t)}-\mathbf{A}_3\boldsymbol{\beta}_0(t)-\mathbf{A}_2\boldsymbol{\beta}_1(t)-\mathbf{A}_1\boldsymbol{\beta}_2(t)+f_3\left(\frac{\mathrm{d}\boldsymbol{\beta}_1(t)}{\mathrm{d}t},\frac{\mathrm{d}\boldsymbol{\beta}_2(t)}{\mathrm{d}t}\right),$$

$$\vdots$$

$$\boldsymbol{\beta}_p(t)=\boldsymbol{\sigma}_0(t)-\mathbf{A}_p\boldsymbol{\beta}_0(t)-\mathbf{A}_{p-1}\boldsymbol{\beta}_1(t)-\cdots-\mathbf{A}_1\boldsymbol{\beta}_{p-1}(t)+f_p\left(\frac{\mathrm{d}\boldsymbol{\beta}_1(t)}{\mathrm{d}t},\ldots,\frac{\mathrm{d}\boldsymbol{\beta}_{p-1}(t)}{\mathrm{d}t}\right),$$

where $f_2(\mathrm{d}\boldsymbol{\beta}_1(t)/\mathrm{d}t)$ is the function with respect to $\mathrm{d}\boldsymbol{\beta}_1(t)/\mathrm{d}t$.

The state-space model is also called the undetermined coefficient model (see [11]).

The stochastic differential equation (3) has the following strong solution (see Ref. [12, Section 5.6]):

$$\mathbf{Y}(t)=\mathrm{e}^{\mathbf{A}(t-t_0)}\mathbf{Y}(t_0)+\int_{t_0}^{t}\mathrm{e}^{\mathbf{A}(t-s)}\mathbf{J}(s)\,\mathrm{d}s+\int_{t_0}^{t}\mathrm{e}^{\mathbf{A}(t-s)}\mathbf{C}(s)\,\mathrm{d}\mathbf{W}(s), \tag{4}$$

where $\mathrm{e}^{\mathbf{A}t}=\mathbf{I}_n+\sum_{k=1}^{\infty}(\mathbf{A}t)^k/k!$, t_0 denotes the initial time. For a special circumstance t_0=0, we have

$$\mathbf{Y}(t)=\mathrm{e}^{\mathbf{A}t}\mathbf{Y}(0)+\int_{0}^{t}\mathrm{e}^{\mathbf{A}(t-s)}\mathbf{J}(s)\,\mathrm{d}s+\int_{0}^{t}\mathrm{e}^{\mathbf{A}(t-s)}\mathbf{C}(s)\,\mathrm{d}\mathbf{W}(s). \tag{5}$$

Assuming that the initial state $\mathbf{Y}(0)$ has an n-dimensional normal distribution and is independent of $\mathbf{W}(t)$, then the response process $\mathbf{Y}(t)$ is Gaussian too and it is completely defined from a probabilistic point of view by the knowledge of the statistics up to second order, i.e. the mean vector and the covariance matrix. The mean vector and covariance matrix, for every $0\le t<\infty$, are expressed as

$$E(\mathbf{Y}(t))=\mathrm{e}^{\mathbf{A}t}E(\mathbf{Y}(0))+\int_0^t\mathrm{e}^{\mathbf{A}(t-s)}\mathbf{J}(s)\,\mathrm{d}s,$$

$$\mathrm{Var}(\mathbf{Y}(t))=\mathrm{e}^{\mathbf{A}t}\,\mathrm{Var}(\mathbf{Y}(0))\mathrm{e}^{\mathbf{A}^{\mathrm{T}}t}+\int_0^t\mathrm{e}^{\mathbf{A}(t-s)}\mathbf{C}(s)\mathbf{C}^{\mathrm{T}}(s)\mathrm{e}^{\mathbf{A}^{\mathrm{T}}(t-s)}\,\mathrm{d}s.$$

Let $\mathbf{S}(t)=\mathbf{Y}(t)-E(\mathbf{Y}(t))$, then

$$\begin{aligned}\mathrm{d}\mathbf{S}(t)&=\mathrm{d}\mathbf{Y}(t)-\mathrm{d}\left(\mathrm{e}^{\mathbf{A}t}E(\mathbf{Y}(0))+\int_0^t\mathrm{e}^{\mathbf{A}(t-s)}\mathbf{J}(s)\,\mathrm{d}s\right)=\mathrm{d}\mathbf{Y}(t)-\mathbf{A}\mathrm{e}^{\mathbf{A}t}E(\mathbf{Y}(0))\,\mathrm{d}t-\mathbf{J}(t)\,\mathrm{d}t\\&-\left[\int_0^t\mathbf{A}\mathrm{e}^{\mathbf{A}(t-s)}\mathbf{J}(s)\,\mathrm{d}s\right]\mathrm{d}t=\mathbf{A}\mathbf{Y}(t)\,\mathrm{d}t+\mathbf{J}(t)\,\mathrm{d}t+\mathbf{C}(t)\,\mathrm{d}\mathbf{W}(t)-\mathbf{A}\mathrm{e}^{\mathbf{A}t}E(\mathbf{Y}(0))\,\mathrm{d}t-\mathbf{J}(t)\,\mathrm{d}t\\&-\left[\int_0^t\mathbf{A}\mathrm{e}^{\mathbf{A}(t-s)}\mathbf{J}(s)\,\mathrm{d}s\right]\mathrm{d}t=\mathbf{A}\left[\mathbf{Y}(t)-\mathrm{e}^{\mathbf{A}t}E(\mathbf{Y}(0))-\int_0^t\mathrm{e}^{\mathbf{A}(t-s)}\mathbf{J}(s)\,\mathrm{d}s\right]\mathrm{d}t+\mathbf{C}(t)\,\mathrm{d}\mathbf{W}(t)\\&=\mathbf{A}[\mathbf{Y}(t)-E(\mathbf{Y}(t))]\,\mathrm{d}t+\mathbf{C}(t)\,\mathrm{d}\mathbf{W}(t)=\mathbf{A}\mathbf{S}(t)\,\mathrm{d}t+\mathbf{C}(t)\,\mathrm{d}\mathbf{W}(t).\end{aligned}$$

For notational convenience, we still denote the difference $\mathbf{Y}(t)-E(\mathbf{Y}(t))$ as $\mathbf{Y}(t)$, so one can obtain the concisely stochastic differential equation

$$\mathrm{d}\mathbf{Y}(t)=\mathbf{A}\mathbf{Y}(t)\,\mathrm{d}t+\mathbf{C}(t)\,\mathrm{d}\mathbf{W}(t). \tag{6}$$

Therefore, in later sections, we always assume that $\mathbf{Y}(t)$ satisfies Eq. (6).

When the order q in the CARMA(p,q) model is zero, the CARMA(p,q) model is also called the CAR(p) model.

3. The CARMA representation of a vibratory system

The structural dynamic equation of an MDOF vibratory system excited by an unknown random Gaussian force can be expressed as

$$\mathbf{M}\ddot{\mathbf{X}}(t)+\mathbf{C}\dot{\mathbf{X}}(t)+\mathbf{K}\mathbf{X}(t)=\mathbf{u}(t), \tag{7}$$

where ($\mathbf{M}$, $\mathbf{C}$ and $\mathbf{K}$ are the $n\times n$ mass, damping and stiffness matrices, respectively; $\ddot{\mathbf{X}}(t)$, $\dot{\mathbf{X}}(t)$ and $\mathbf{X}(t)$ are $n\times 1$ vectors of acceleration, velocity and displacement, respectively, and $\mathbf{u}(t)$ denotes the $n\times 1$ external loading vector.

The ultimate goal of modal analysis is to identify the modal parameters of the system, and then to provide the basis for the vibration characteristics analysis, fault diagnosis, prediction of the structural system and the optimal design of the structural dynamic characteristics. However, in practical engineering applications, structural dynamic modification and dynamic design are all implemented through the physical parameters rather than modal parameters. So in order to meet the structural needs, we eventually need to measure the physical parameters of the structure.In many cases of practical interest, the masses of a system can be estimated more accurately. Hence, we assume that the mass matrix $\mathbf{M}$ is known, and only $\mathbf{K}$ and $\mathbf{C}$ need to be identified, and we assume the system is excited by wind load.

In Ref. [13], Harris presented the expression of wind load at height z,

$$P(z,t)=\overline{v}(z)+v_f(t),$$

where $\overline{v}(z)$ is the mean wind velocity at height z and $v_f(t)$ denotes the pulsation wind. The inherent non-stationarity of wind load means the non-stationarity of $v_f(t)$. In general cases, $v_f(t)$ is Gaussian too.

If the random excitation is a non-stationary random perturbation (noise), then $v_f(t)$ can be written by $v_f(t)=\lambda_1(t)+\eta(t)DW(t)$, where $\lambda_1(t)$ denotes the trend term of the random excitation. Based on $v_f(t)$ and the expression of $P(z,t)$, one can obtain

$$P(z,t)=\lambda(z,t)+\eta(t)DW(t), \tag{8}$$

where $\lambda(z,t)$ is the combination of $\overline{v}(z)$ and $\lambda_1(t)$.

By virtue of Eq. (8), the non-stationary random excitation vector $\mathbf{u}(t)$ in Eq. (7) can be expressed by $\mathbf{u}(t)=\boldsymbol{\lambda}(t)+\boldsymbol{\eta}(t)D\mathbf{W}(t)$, where $\boldsymbol{\lambda}(t)$ is a column vector, $\{\mathbf{W}(t)\}$ is an n-dimensional Brownian motion and $\boldsymbol{\eta}(t)$ is assumed to be a non-singular matrix. So Eq. (7) becomes

$$\mathbf{M}\ddot{\mathbf{X}}(t)+\mathbf{C}\dot{\mathbf{X}}(t)+\mathbf{K}\mathbf{X}(t)=\boldsymbol{\lambda}(t)+\boldsymbol{\eta}(t)D\mathbf{W}(t).$$

If random excitation is covariance non-stationary, it is natural to think of describing it by a continuous time MA model due to the time dependence of the MA model. If we further restrict the order of the MA model to 1, then the structural dynamic equation can be expressed as

$$\ddot{\mathbf{X}}(t)+\mathbf{A}_1\dot{\mathbf{X}}(t)+\mathbf{A}_2\mathbf{X}(t)=\boldsymbol{\lambda}(t)+\boldsymbol{\eta}_0(t)D\mathbf{W}(t)+\boldsymbol{\eta}_1(t)D^2\mathbf{W}(t). \tag{9}$$

The above conclusion shows that under some restricted conditions, the structural dynamic equation is essentially a CARMA model. Once the parameters of the CARMA model are identified, we can obtain the modal parameters by the eigenvalue analysis method.

The CARMA model differs from the traditional time series models in that it is a continuous time ARMA model, and it overcomes the deficiencies, such as the lower computing efficiency, the strong dependence on initial parameters and the higher complexity on the MDOF system, of the discrete time ARMA models.

4. Parameter estimation

In order to give a more full understanding on the modal identification method of the CARMA model, we first introduce the simpler one of the CAR model.

4.1. Parameter estimation for the CAR model

4.1.1. Parameter estimation when $\boldsymbol{\sigma}(t)$ is an identity matrix

The following method was presented firstly by Brockwell et al. [14] in 2007. In his paper, the estimation of parameters of the simple degree-of-freedom system was presented under the assumption that the uniformly modulated function is a constant. In this section, we extend the method to the case of an MDOF system.

Eq. (6) can be expressed as

$$\begin{aligned}
\mathrm{d}\mathbf{Y}_0(t)&=\mathbf{Y}_1(t)\,\mathrm{d}t,\\
\mathrm{d}\mathbf{Y}_1(t)&=\mathbf{Y}_2(t)\,\mathrm{d}t,\\
&\vdots\\
\mathrm{d}\mathbf{Y}_{p-2}(t)&=\mathbf{Y}_{p-1}(t)\,\mathrm{d}t,\\
\mathrm{d}\mathbf{Y}_{p-1}(t)&=[-\mathbf{A}_p\mathbf{Y}_0(t)-\cdots-\mathbf{A}_1\mathbf{Y}_{p-1}(t)]\,\mathrm{d}t+\mathrm{d}\mathbf{W}(t).
\end{aligned} \tag{10}$$

We see from the first $p-1$ rows of Eq. (10) that $\mathbf{Y}_j(t)$ $(j=0,\ldots,p-2)$ is the function with respect to both $\mathbf{Y}_{p-1}(t)$ and the initial state. Assume that the initial state is expressed by $\mathbf{Y}(0)=(\mathbf{y}_0^{\mathrm{T}},\ldots,\mathbf{y}_{p-1}^{\mathrm{T}})^{\mathrm{T}}$, the last equation in Eq. (10) can be written in the form like

$$\mathrm{d}\mathbf{Y}_{p-1}(t)=\mathbf{G}(\mathbf{Y}_{p-1},t)\,\mathrm{d}t+\mathrm{d}\mathbf{W}(t), \tag{11}$$

where $\mathbf{G}(\mathbf{Y}_{p-1},t)$ is an n-dimensional function with respect to $\{\mathbf{Y}_{p-1}(s),0\le s\le t\}$.

Now let us begin with an n-dimensional Brownian motion $\mathbf{W}(t)$ (with $\mathbf{W}(0)=\mathbf{y}_{p-1}$) defined on the probability space $(C[0,T]^n,\mathcal{B}(C[0,T]^n),P_{\mathbf{y}_{p-1}})$. For $t\le T$, let $\mathcal{F}_t=\sigma(\mathbf{W}(s),s\le t)\vee\mathcal{N}$, where $\mathcal{N}$ is the $\sigma-$algebra of $P_{\mathbf{y}_{p-1}}-$null sets of $\mathcal{B}(C[0,T]^n)$. Equations

$$\begin{aligned}
\mathrm{d}\mathbf{Z}_0(t)&=\mathbf{Z}_1(t)\,\mathrm{d}t,\\
\mathrm{d}\mathbf{Z}_1(t)&=\mathbf{Z}_2(t)\,\mathrm{d}t,\\
&\vdots
\end{aligned}$$

$$\mathrm{d}\mathbf{Z}_{p-2}(t)=\mathbf{Z}_{p-1}(t)\,\mathrm{d}t,$$

$$\mathrm{d}\mathbf{Z}_{p-1}(t)=\mathrm{d}\mathbf{W}(t),$$

with $\mathbf{Z}(0)$=$\mathbf{Y}(0)$, clearly have the unique strong solution. Indeed, by Definition 5.2.3 of Karatzas and Shreve (see [12]), for any two processes $\mathbf{Z}^{(1)}_{p-1}(t)$ and $\mathbf{Z}^{(2)}_{p-1}(t)$ satisfying the above equation, we may observe that

$$\mathbf{Z}^{(i)}_{p-1}(t)=\mathbf{y}_{p-1}(0)+\mathbf{W}(t),\quad 0\le t\le T,\ i=1,2,$$

which means $\mathbf{Z}^{(1)}_{p-1}(t)=\mathbf{Z}^{(2)}_{p-1}(t)$, a.s.

Obviously, $\mathbf{G}(\mathbf{Z}_{p-1},t)$ is adapted to the filtration $\mathcal{F}_t$. One can also verify that $\int_0^T \|\mathbf{G}(\mathbf{Z}_{p-1},t)\|^2\,\mathrm{d}t<\infty$ almost surely, where the notation $\|\cdot\|$ represents the Euclidean norm of a vector. Let

$$L_t\triangleq\exp\left\{\int_0^t(\mathbf{G}(\mathbf{Z}_{p-1},s))^{\mathrm{T}}\,\mathrm{d}\mathbf{W}(s)-\frac{1}{2}\int_0^t\|\mathbf{G}(\mathbf{Z}_{p-1},s)\|^2\,\mathrm{d}s\right\},$$

then L_t is a martingale under probability measure $P_{\mathbf{y}_{p-1}}$, so the Girsanov Theorem 3.5.1 (see [12]) implies that, under the probability $\tilde{P}_T$ given by $\mathrm{d}\tilde{P}_T/\mathrm{d}P_{\mathbf{y}_{p-1}}=L_T$, the process

$$\tilde{\mathbf{W}}(t)\triangleq\mathbf{W}(t)-\int_0^t\mathbf{G}(\mathbf{Z}_{p-1},s)\,\mathrm{d}s,\quad 0\le t\le T$$

is an n-dimensional Brownian motion. Hence by Propositions 5.3.6 and 5.3.10 of Karatzas and Shreve (see [12]), we see that Eq. (6) with initial condition $\mathbf{Y}(0)$ have, for $0\le t\le T$, the weak solutions $(\mathbf{Z}_{p-1}(t),\tilde{\mathbf{W}}(t))$ and $(\mathbf{Y}(t),\ \mathbf{W}(t))$, and the weak solutions are unique in law, and by Theorem 10.2.2 of Stroock and Varadhan (see [15]), they are non-explosive.

If f is a bounded measurable functional on $C[0,T]^n$, then

$$\tilde{E}f(\mathbf{Z}_{p-1})=E_{\mathbf{y}_{p-1}}[f(\mathbf{Z}_{p-1})L_T]=\int f(\xi)L_T(\xi)\,\mathrm{d}P_{\mathbf{y}_{p-1}}(\xi).$$

In other words, L_T is the density, conditional on $\mathbf{y}_{p-1}$, of $\mathbf{Y}_{p-1}(t)$ with respect to measure $P_{\mathbf{y}_{p-1}}$. If we can observe $\mathbf{Y}_{p-1}$, then we could compute the conditional maximum likelihood estimators of the unknown parameters by maximizing L_T. Estimators via this method are called exact maximum likelihood estimators.

For the CAR(p) process defined by Eq. (6), denoting the realized state process on $[0,T]$ by $\{\mathbf{y}(s)=(\mathbf{z}_0^{\mathrm{T}}(s),\ldots,\mathbf{z}_{p-1}^{\mathrm{T}}(s))^{\mathrm{T}},0\le s\le T\}$, we have

$$\log L_T=\int_0^T\mathbf{G}^{\mathrm{T}}\,\mathrm{d}\mathbf{z}_{p-1}(s)-\frac{1}{2}\int_0^T\mathbf{G}^{\mathrm{T}}\,\mathbf{G}\,\mathrm{d}s. \tag{12}$$

Differentiating Eq. (12) with respect to $\mathbf{A}_1,\ldots,\mathbf{A}_p$ and setting the derivatives equal to zero give the exact maximum likelihood estimators of parameters:

$$\widehat{(\mathbf{A}_1,\ldots,\mathbf{A}_p)}=-\left(\int_0^T\mathrm{d}\mathbf{z}_{p-1}(\mathbf{z}_{p-1}^{\mathrm{T}},\ldots,\mathbf{z}_0^{\mathrm{T}})\right)\left(\int_0^T(\mathbf{z}_{p-1}^{\mathrm{T}},\ldots,\mathbf{z}_0^{\mathrm{T}})^{\mathrm{T}}(\mathbf{z}_{p-1}^{\mathrm{T}},\ldots,\mathbf{z}_0^{\mathrm{T}})\,\mathrm{d}t\right)^{-1}. \tag{13}$$

4.1.2. Estimation for $\boldsymbol{\sigma}(t)$

For many non-stationary cases, the uniform modulated function $\boldsymbol{\sigma}(t)$ is not an identity matrix, so it is necessary to estimate $\boldsymbol{\sigma}(t)$ firstly.

Eq. (4) can be written in the following form:

$$\mathbf{Y}(t)-\mathrm{e}^{\mathbf{A}(t-t_0)}\mathbf{Y}(t_0)=\int_{t_0}^t\mathrm{e}^{\mathbf{A}(t-s)}\mathbf{C}(s)\,\mathrm{d}\mathbf{W}(s). \tag{14}$$

For any $h>0$, replacing t with $t+h$ and t_0 with t, squaring and taking expectation on both sides of Eq. (14), we have

$$E(\mathbf{Y}(t+h)-\mathrm{e}^{\mathbf{A}h}\mathbf{Y}(t))(\mathbf{Y}(t+h)-\mathrm{e}^{\mathbf{A}h}\mathbf{Y}(t))^{\mathrm{T}}=\int_t^{t+h}\mathrm{e}^{\mathbf{A}(t+h-s)}\mathbf{C}(s)\mathbf{C}^{\mathrm{T}}(s)\mathrm{e}^{\mathbf{A}^{\mathrm{T}}(t+h-s)}\,\mathrm{d}s=\int_0^h\mathrm{e}^{\mathbf{A}(h-u)}\mathbf{C}(u+t)\mathbf{C}^{\mathrm{T}}(u+t)\mathrm{e}^{\mathbf{A}^{\mathrm{T}}(h-u)}\,\mathrm{d}u. \tag{15}$$

Since the interest here is to discuss the modal identification of structural systems, we only need to identify the parameters of the CAR(2) model. For the CAR(2) model,

$$\mathbf{A}=\begin{pmatrix}\mathbf{0}&\mathbf{I}_n\\-\mathbf{A}_2&-\mathbf{A}_1\end{pmatrix},\quad\mathbf{C}(t)=\begin{pmatrix}\mathbf{0}\\\boldsymbol{\sigma}(t)\end{pmatrix}.$$

Let

$$\mathrm{e}^{\mathbf{A}(h-u)}=\begin{pmatrix}\mathbf{H}_{11}(h-u)&\mathbf{H}_{12}(h-u)\\\mathbf{H}_{21}(h-u)&\mathbf{H}_{22}(h-u)\end{pmatrix},$$

where $\mathbf{H}_{ij}$ $(i,j=1,2)$ is the n-dimensional square matrix, then Eq. (15) can be written as

$$E(\mathbf{Y}(t+h)-e^{\mathbf{A}h}\mathbf{Y}(t))(\mathbf{Y}(t+h)-e^{\mathbf{A}h}\mathbf{Y}(t))^{\mathrm{T}}=\begin{pmatrix}\int_0^h \mathbf{H}_{12}\boldsymbol{\sigma}(u+t)\boldsymbol{\sigma}^{\mathrm{T}}(u+t)\mathbf{H}_{12}^{\mathrm{T}}\,\mathrm{d}u & \int_0^h \mathbf{H}_{12}\boldsymbol{\sigma}(u+t)\boldsymbol{\sigma}^{\mathrm{T}}(u+t)\mathbf{H}_{22}^{\mathrm{T}}\,\mathrm{d}u\\ \int_0^h \mathbf{H}_{22}\boldsymbol{\sigma}(u+t)\boldsymbol{\sigma}^{\mathrm{T}}(u+t)\mathbf{H}_{12}^{\mathrm{T}}\,\mathrm{d}u & \int_0^h \mathbf{H}_{22}\boldsymbol{\sigma}(u+t)\boldsymbol{\sigma}^{\mathrm{T}}(u+t)\mathbf{H}_{22}^{\mathrm{T}}\,\mathrm{d}u\end{pmatrix}. \tag{16}$$

Generally, the uniformly modulated function $\boldsymbol{\sigma}(t)$ is continuous on the observed interval $[0,T]$, therefore, there exists a sequence $\{t_i\}$ of real numbers with $0=t_0<t_1<\cdots<t_k=T$ which can divide $[0,T]$ into k consecutive subintervals $T_1,\ldots,T_k$, and $\boldsymbol{\sigma}(t)$ is considered as nearly constant matrix (denoted as $\boldsymbol{\sigma}(t_i)$) on the subinterval T_i $(i=1,\ldots,k)$.

Now let us consider the ith subinterval T_i. Given $h>0$ and $h\to 0$, we can divide T_i into $m=|T_i|/h$ consecutive sub-subintervals $[t_i,t_i+h],\ldots,[t_i+(m-1)h,t_i+mh]$. For sub-subintervals $[t_i,t_i+h],\ldots,[t_i+(m-1)h,t_i+mh]$, the right side terms of Eq. (16) are identical and are the function with respect to $\boldsymbol{\sigma}(t_i)$, so the expectation of Eq. (16) can be estimated by the corresponding sample moment, namely,

$$\frac{\sum_{j=1}^{m}(\mathbf{Y}(t_i+jh)-e^{\mathbf{A}h}\mathbf{Y}(t_i+(j-1)h))(\mathbf{Y}(t_i+jh)-e^{\mathbf{A}h}\mathbf{Y}(t_i+(j-1)h))^{\mathrm{T}}}{m}\triangleq\begin{pmatrix}\mathbf{V}_{11} & \mathbf{V}_{12}\\ \mathbf{V}_{21} & \mathbf{V}_{22}\end{pmatrix}.$$

Therefore, on the interval T_i, the estimator of Eq. (16) is

$$\widehat{\begin{pmatrix}\int_0^h \mathbf{H}_{12}\boldsymbol{\sigma}(t_i)\boldsymbol{\sigma}^{\mathrm{T}}(t_i)\mathbf{H}_{12}^{\mathrm{T}}\,\mathrm{d}u & \int_0^h \mathbf{H}_{12}\boldsymbol{\sigma}(t_i)\boldsymbol{\sigma}^{\mathrm{T}}(t_i)\mathbf{H}_{22}^{\mathrm{T}}\,\mathrm{d}u\\ \int_0^h \mathbf{H}_{22}\boldsymbol{\sigma}(t_i)\boldsymbol{\sigma}^{\mathrm{T}}(t_i)\mathbf{H}_{12}^{\mathrm{T}}\,\mathrm{d}u & \int_0^h \mathbf{H}_{22}\boldsymbol{\sigma}(t_i)\boldsymbol{\sigma}^{\mathrm{T}}(t_i)\mathbf{H}_{22}^{\mathrm{T}}\,\mathrm{d}u\end{pmatrix}}=\begin{pmatrix}\mathbf{V}_{11} & \mathbf{V}_{12}\\ \mathbf{V}_{21} & \mathbf{V}_{22}\end{pmatrix}. \tag{17}$$

However, $\boldsymbol{\sigma}(t_i)$ only contains $n\times n$ parameters, while Eq. (17) contains $2n\times 2n$ equations, which will lead to redundance. Therefore, only by solving the following equation can obtain the estimator of $\boldsymbol{\sigma}(t_i)$:

$$\int_0^h \mathbf{H}_{22}\boldsymbol{\sigma}(t_i)\boldsymbol{\sigma}^{\mathrm{T}}(t_i)\mathbf{H}_{22}^{\mathrm{T}}\,\mathrm{d}u=\mathbf{V}_{22}. \tag{18}$$

Obviously, Eq. (18) is a nonlinear function of the parameter $\boldsymbol{\sigma}(t_i)$, so a nonlinear algorithm is needed. The following are only several computing formulas for some especial cases in practical applications.

1. $\boldsymbol{\sigma}(t_i)$ is a diagonal matrix.

The assumption applies to the case that the random excitation is space-uncorrelated.

Assuming $\boldsymbol{\sigma}(t_i)=\mathrm{diag}(\sigma_1,\ldots,\sigma_n)$ is a constant matrix on the interval T_i. If we choose the diagonal elements of $\int_0^h \mathbf{H}_{22}\boldsymbol{\sigma}(t_i)\boldsymbol{\sigma}^{\mathrm{T}}(t_i)\mathbf{H}_{22}^{\mathrm{T}}\,\mathrm{d}u$ to construct a column vector, and the diagonal elements of $\mathbf{V}_{22}$ to construct the column vector $(v_{11},\ldots,v_{nn})^{\mathrm{T}}$, then from Eq. (18), we have

$$\begin{pmatrix}v_{11}\\ v_{22}\\ \vdots\\ v_{nn}\end{pmatrix}=\begin{pmatrix}\int_0^h h_{11}^2\,\mathrm{d}u & \int_0^h h_{12}^2\,\mathrm{d}u & \cdots & \int_0^h h_{1n}^2\,\mathrm{d}u\\ \int_0^h h_{21}^2\,\mathrm{d}u & \int_0^h h_{22}^2\,\mathrm{d}u & \cdots & \int_0^h h_{2n}^2\,\mathrm{d}u\\ \vdots & \vdots & \cdots & \vdots\\ \int_0^h h_{n1}^2\,\mathrm{d}u & \int_0^h h_{n2}^2\,\mathrm{d}u & \cdots & \int_0^h h_{nn}^2\,\mathrm{d}u\end{pmatrix}\begin{pmatrix}\sigma_1^2\\ \sigma_2^2\\ \vdots\\ \sigma_n^2\end{pmatrix}, \tag{19}$$

where $h_{ij}=h_{ij}(h-u)$ $(i,j=1,\ldots,n)$ denotes the (i,j)th element of $\mathbf{H}_{22}$. Therefore, from Eq. (19), one can obtain the estimator of $\boldsymbol{\sigma}^2(t_i)$ on the interval T_i:

$$\begin{pmatrix}\widehat{\sigma}_1^2\\ \widehat{\sigma}_2^2\\ \vdots\\ \widehat{\sigma}_n^2\end{pmatrix}=\begin{pmatrix}\int_0^h h_{11}^2\,\mathrm{d}u & \int_0^h h_{12}^2\,\mathrm{d}u & \cdots & \int_0^h h_{1n}^2\,\mathrm{d}u\\ \int_0^h h_{21}^2\,\mathrm{d}u & \int_0^h h_{22}^2\,\mathrm{d}u & \cdots & \int_0^h h_{2n}^2\,\mathrm{d}u\\ \vdots & \vdots & \cdots & \vdots\\ \int_0^h h_{n1}^2\,\mathrm{d}u & \int_0^h h_{n2}^2\,\mathrm{d}u & \cdots & \int_0^h h_{nn}^2\,\mathrm{d}u\end{pmatrix}^{-1}\begin{pmatrix}v_{11}\\ v_{22}\\ \vdots\\ v_{nn}\end{pmatrix}. \tag{20}$$

In the above computation process, we need to know the sub-matrix $\mathbf{H}_{22}$ of $e^{\mathbf{A}h}$, which is unknown because $\mathbf{A}$ is an unknown parameter. However, when h tends to 0 and $\mathbf{A}$ has the form in Section 3, $e^{\mathbf{A}h}$ is nearly a constant matrix. So we can use the raw estimator of $\mathbf{A}$ obtained in Section 4.1.1 as the initial value to compute $e^{\mathbf{A}h}$, then obtain the estimator of $\boldsymbol{\sigma}(t_i)$ from the above equation. Finally, the estimator of $\boldsymbol{\sigma}(t)$ can be obtained by spline interpolation of $\widehat{\boldsymbol{\sigma}}(t_i)$ $(i=1,\ldots,k)$.

2. $\boldsymbol{\sigma}(t_i)$ is a special block diagonal matrix.

The assumption applies to the case that the random excitation is space-correlated.

Assuming $\boldsymbol{\sigma}(t_i)$ is expressed as

$$\begin{pmatrix} \begin{matrix} \sigma_1 & 0 & \cdots & 0 \\ \sigma_2 & 0 & \cdots & 0 \\ \vdots & \vdots & \cdots & \vdots \\ \sigma_l & 0 & \cdots & 0 \end{matrix} & & & \\ & \begin{matrix} \sigma_{l+1} & 0 & \cdots & 0 \\ \vdots & \vdots & \cdots & \vdots \\ \sigma_{2l} & 0 & \cdots & 0 \end{matrix} & & \\ & & \ddots & \\ & & & \begin{matrix} \sigma_{jl+1} & 0 & \cdots & 0 \\ \vdots & \vdots & \cdots & \vdots \\ \sigma_n & 0 & \cdots & 0 \end{matrix} \end{pmatrix},$$

where the main diagonal of $\boldsymbol{\sigma}(t_i)$ includes $j=\mathrm{mod}(n,l)$ or $j=\mathrm{mod}(n,l)+1$ sub-matrices.

Let

$$C=\left(\begin{matrix}
\int_0^h h_{11}^2\,\mathrm{d}u & \cdots & \int_0^h h_{1n}^2\,\mathrm{d}u & 2\int_0^h h_{11}h_{12}\,\mathrm{d}u & \cdots \\
\vdots & \cdots & \vdots & \vdots & \cdots \\
\int_0^h h_{n1}^2\,\mathrm{d}u & \cdots & \int_0^h h_{nn}^2\,\mathrm{d}u & 2\int_0^h h_{n1}h_{n2}\,\mathrm{d}u & \cdots \\
\int_0^h h_{11}h_{21}\,\mathrm{d}u & \cdots & \int_0^h h_{1n}h_{2n}\,\mathrm{d}u & \int_0^h (h_{12}h_{21}+h_{11}h_{22})\,\mathrm{d}u & \cdots \\
\vdots & \cdots & \vdots & \vdots & \cdots \\
\int_0^h h_{11}h_{n1}\,\mathrm{d}u & \cdots & \int_0^h h_{1n}h_{nn}\,\mathrm{d}u & \int_0^h (h_{12}h_{n1}+h_{11}h_{n2})\,\mathrm{d}u & \cdots \\
\int_0^h h_{21}h_{31}\,\mathrm{d}u & \cdots & \int_0^h h_{2n}h_{3n}\,\mathrm{d}u & \int_0^h (h_{22}h_{31}+h_{21}h_{32})\,\mathrm{d}u & \cdots \\
\vdots & \cdots & \vdots & \vdots & \cdots \\
\int_0^h h_{21}h_{n1}\,\mathrm{d}u & \cdots & \int_0^h h_{2n}h_{nn}\,\mathrm{d}u & \int_0^h (h_{22}h_{n1}+h_{21}h_{n2})\,\mathrm{d}u & \cdots \\
\vdots & \cdots & \vdots & \vdots & \cdots \\
\int_0^h h_{(n-1)1}h_{n1}\,\mathrm{d}u & \cdots & \int_0^h h_{(n-1)n}h_{nn}\,\mathrm{d}u & \int_0^h (h_{(n-1)2}h_{n1}+h_{(n-1)1}h_{n2})\,\mathrm{d}u & \cdots
\end{matrix}\right.$$

$$\begin{matrix}
2\int_0^h h_{11}h_{1n}\,\mathrm{d}u & \int_0^h 2h_{12}h_{13}\,\mathrm{d}u & \cdots \\
\vdots & \vdots & \cdots \\
2\int_0^h h_{n1}h_{nn}\,\mathrm{d}u & \int_0^h 2h_{n2}h_{n3}\,\mathrm{d}u & \cdots \\
\int_0^h (h_{1n}h_{21}+h_{11}h_{2n})\,\mathrm{d}u & \int_0^h (h_{13}h_{22}+h_{12}h_{23})\,\mathrm{d}u & \cdots \\
\vdots & \vdots & \cdots \\
\int_0^h (h_{1n}h_{n1}+h_{11}h_{nn})\,\mathrm{d}u & \int_0^h (h_{13}h_{n2}+h_{12}h_{n3})\,\mathrm{d}u & \cdots \\
\int_0^h (h_{2n}h_{31}+h_{21}h_{3n})\,\mathrm{d}u & \int_0^h (h_{23}h_{32}+h_{22}h_{33})\,\mathrm{d}u & \cdots \\
\vdots & \vdots & \cdots \\
\int_0^h (h_{2n}h_{n1}+h_{21}h_{nn})\,\mathrm{d}u & \int_0^h (h_{23}h_{n2}+h_{22}h_{n3})\,\mathrm{d}u & \cdots \\
\vdots & \vdots & \cdots \\
\int_0^h (h_{(n-1)n}h_{n1}+h_{(n-1)1}h_{nn})\,\mathrm{d}u & \int_0^h (h_{(n-1)3}h_{n2}+h_{(n-1)2}h_{n3})\,\mathrm{d}u & \cdots
\end{matrix}$$

$$\left.\begin{matrix}
\int_0^h 2h_{12}h_{1n}\,\mathrm{d}u & \cdots & \int_0^h 2h_{1(n-1)}h_{1n}\,\mathrm{d}u \\
\vdots & \cdots & \vdots \\
\int_0^h 2h_{n2}h_{nn}\,\mathrm{d}u & \cdots & \int_0^h 2h_{n(n-1)}h_{nn}\,\mathrm{d}u \\
\int_0^h (h_{1n}h_{22}+h_{12}h_{2n})\,\mathrm{d}u & \cdots & \int_0^h (h_{1n}h_{2(n-1)}+h_{1(n-1)}h_{2n})\,\mathrm{d}u \\
\vdots & \cdots & \vdots \\
\int_0^h (h_{1n}h_{n2}+h_{12}h_{nn})\,\mathrm{d}u & \cdots & \int_0^h (h_{1n}h_{n(n-1)}+h_{1(n-1)}h_{nn})\,\mathrm{d}u \\
\int_0^h (h_{2n}h_{32}+h_{22}h_{3n})\,\mathrm{d}u & \cdots & \int_0^h (h_{2n}h_{3(n-1)}+h_{2(n-1)}h_{3n})\,\mathrm{d}u \\
\vdots & \cdots & \vdots \\
\int_0^h (h_{2n}h_{n2}+h_{22}h_{nn})\,\mathrm{d}u & \cdots & \int_0^h (h_{2n}h_{n(n-1)}+h_{2(n-1)}h_{nn})\,\mathrm{d}u \\
\vdots & \cdots & \vdots \\
\int_0^h (h_{(n-1)n}h_{n2}+h_{(n-1)2}h_{nn})\,\mathrm{d}u & \cdots & \int_0^h (h_{(n-1)n}h_{n(n-1)}+h_{(n-1)(n-1)}h_{nn})\,\mathrm{d}u
\end{matrix}\right),$$

$$V=(v_{11},\ldots,v_{nn},v_{12},\ldots,v_{1n},v_{23},\ldots,v_{2n},\ldots,v_{(n-1)n})^{\mathrm{T}},$$

then the first n rows of $C^{-1}V$ give the estimator of $\boldsymbol{\sigma}^2(t_i)$. Finally the estimator of $\boldsymbol{\sigma}(t)$ can be obtained by spline interpolation of $\widehat{\boldsymbol{\sigma}}(t_i)$ $(i=1,\ldots,k)$.

When $l>1$, the determinant of the above matrix $\boldsymbol{\sigma}(t_i)$ is zero, so $\boldsymbol{\sigma}(t_i)$ is singular. However, the parameter identification method in Section 4.1.3 requires the non-singularity of $\boldsymbol{\sigma}(t_i)$. Therefore, we present a new method, that is, constructing the new matrix

$$\boldsymbol{\sigma}_1(t_i)=\begin{pmatrix} B_1 & & & \\ & B_2 & & \\ & & \ddots & \\ & & & B_j \end{pmatrix},$$

where

$$B_i=\begin{pmatrix} \sigma_{(i-1)l+1} & 0 & \cdots & 0 \\ \sigma_{(i-1)l+2} & p\sigma_{(i-1)l+2} & \cdots & 0 \\ \vdots & \vdots & \cdots & \vdots \\ \sigma_{il} & 0 & \cdots & p\sigma_{il} \end{pmatrix} \quad (i=1,\ldots,j)$$

to adjust $\boldsymbol{\sigma}(t_i)$. When p is small enough, $\boldsymbol{\sigma}_1(t_i)$ is quite close to $\boldsymbol{\sigma}(t_i)$, and $\boldsymbol{\sigma}_1(t_i)$ is non-singular.

3. $\boldsymbol{\sigma}(t_i)$ is the lower triangular matrix.

When h tends to 0, $E(\mathbf{Y}(t+h)-\mathrm{e}^{\mathbf{A}h}\mathbf{Y}(t))(\mathbf{Y}(t+h)-\mathrm{e}^{\mathbf{A}h}\mathbf{Y}(t))^{\mathrm{T}} \approx \mathrm{e}^{\mathbf{A}h}\mathbf{C}\mathbf{C}^{\mathrm{T}}\mathrm{e}^{\mathbf{A}^{\mathrm{T}}h}h$, thus,

$$\mathbf{C}\mathbf{C}^{\mathrm{T}}=\mathrm{e}^{-\mathbf{A}h}E(\mathbf{Y}(t+h)-\mathrm{e}^{\mathbf{A}h}\mathbf{Y}(t))(\mathbf{Y}(t+h)-\mathrm{e}^{\mathbf{A}h}\mathbf{Y}(t))^{\mathrm{T}}\mathrm{e}^{-\mathbf{A}^{\mathrm{T}}h}/h.$$

In fact, $\mathbf{A}$ is the unknown parameter, but when h tends to 0 and $\mathbf{A}$ has the form in Section 3, the sub-matrices $\mathbf{H}_{11}$ and $\mathbf{H}_{22}$ of $\mathrm{e}^{\mathbf{A}h}$ always approximate to the identity matrices, and $\mathbf{H}_{12}$ always approximates to the zero matrix, so

$$\mathrm{e}^{-\mathbf{A}h}\approx\begin{pmatrix} \mathbf{H}_{11}^{-1} & \mathbf{0} \\ * & \mathbf{H}_{22}^{-1} \end{pmatrix},$$

so we have

$$\boldsymbol{\sigma}(t_i)\boldsymbol{\sigma}^{\mathrm{T}}(t_i)=\mathbf{H}_{22}^{-1}\mathbf{V}_{22}\mathbf{H}_{22}^{-\mathrm{T}}/h.$$

When $\boldsymbol{\sigma}(t_i)$ is the lower triangular matrix, estimating $\boldsymbol{\sigma}(t_i)$ means the Cholesky decomposition of $\mathbf{H}_{22}^{-1}\mathbf{V}_{22}\mathbf{H}_{22}^{-\mathrm{T}}/h$, and the decomposition is unique.

4.1.3. Parameter estimation when $\boldsymbol{\sigma}(t)$ is the function of time

Eq. (6) can be expressed as

$$\mathrm{d}\mathbf{Y}_0(t)=\mathbf{Y}_1(t)\,\mathrm{d}t,$$

$$\mathrm{d}\mathbf{Y}_1(t)=\mathbf{Y}_2(t)\,\mathrm{d}t,$$

$$\vdots$$

$$\mathrm{d}\mathbf{Y}_{p-2}(t)=\mathbf{Y}_{p-1}(t)\,\mathrm{d}t,$$

$$\mathrm{d}\mathbf{Y}_{p-1}(t)=[-\mathbf{A}_p\mathbf{Y}_0(t)-\cdots-\mathbf{A}_1\mathbf{Y}_{p-1}(t)]\,\mathrm{d}t+\boldsymbol{\sigma}(t)\,\mathrm{d}\mathbf{W}(t), \tag{21}$$

and

$$\mathrm{d}\mathbf{Y}_{p-1}(t)=\mathbf{G}(\mathbf{Y}_{p-1},t)\,\mathrm{d}t+\boldsymbol{\sigma}(t)\,\mathrm{d}\mathbf{W}(t).$$

Assume $\mathbf{W}(t)$ is an n-dimensional Brownian motion just as in Section 4.1.1, $\mathbf{Z}_{p-1}(t)=\int_0^t\boldsymbol{\sigma}(s)\,\mathrm{d}\mathbf{W}(s)$, $\mathbf{Y}(0)=(\mathbf{y}_0^{\mathrm{T}},\ldots,\mathbf{y}_{p-1}^{\mathrm{T}})^{\mathrm{T}}$. Let us define probability measure $\tilde{P}_T$ and process $\tilde{\mathbf{W}}(t)=\mathbf{W}(t)-\int_0^t\boldsymbol{\sigma}^{-1}(s)\mathbf{G}(\mathbf{Z}_{p-1},s)\,\mathrm{d}s$ as in Section 4.1.1. If $\boldsymbol{\sigma}^{-1}(t)$ exists and is bounded, and let

$$L_t=\exp\left\{\int_0^t(\boldsymbol{\sigma}^{-1}(s)\mathbf{G}(\mathbf{Z}_{p-1},s))^{\mathrm{T}}\,\mathrm{d}\mathbf{W}(s)-\frac{1}{2}\int_0^t\|\boldsymbol{\sigma}^{-1}(t)\mathbf{G}(\mathbf{Z}_{p-1},s)\|^2\,\mathrm{d}s\right\},$$

then L_t is a martingale, and under the probability measure $\tilde{P}_T$, $\{\tilde{\mathbf{W}}(t), 0\le t\le T\}$ is an n-dimensional Brownian motion. So Eq. (6) has the weak solution for $0\le t\le T$, and L_T is the density, conditional on $\mathbf{y}_{p-1}$, of $\mathbf{Y}_{p-1}(t)$ with respect to measure $P_{\mathbf{y}_{p-1}}$. Therefore, we could compute the conditional maximum likelihood estimators of the unknown parameters by maximizing L_T.

The logarithm likelihood function can be expressed as

$$\log L_T=\int_0^T\mathbf{G}^{\mathrm{T}}(\boldsymbol{\sigma}\boldsymbol{\sigma}^{\mathrm{T}})^{-1}(s)\,\mathrm{d}\mathbf{z}_{p-1}(s)-\frac{1}{2}\int_0^T\mathbf{G}^{\mathrm{T}}(\boldsymbol{\sigma}\boldsymbol{\sigma}^{\mathrm{T}})^{-1}(s)\mathbf{G}\,\mathrm{d}s. \tag{22}$$

Differentiating Eq. (22) with respect to $\mathbf{A}_1,\ldots,\mathbf{A}_p$ and setting the derivatives equal to zero give the exact maximum likelihood estimators.

Assuming $\mathbf{P}=(\mathbf{A}_1,\ldots,\mathbf{A}_p)$ is the parameter of the CAR process defined in Section 2. Let $\tilde{\mathbf{Y}}(t)=(\mathbf{z}_{p-1}^{\mathrm{T}}(t),\ldots,\mathbf{z}_0^{\mathrm{T}}(t))^{\mathrm{T}}$, $\tilde{\mathbf{Y}}(t)\tilde{\mathbf{Y}}^{\mathrm{T}}(t)=(\mathbf{a}_1(t),\ldots,\mathbf{a}_{np}(t))\mathbf{R}(t)=(\mathbf{a}_1(t)\otimes(\boldsymbol{\sigma}(t)\boldsymbol{\sigma}^{\mathrm{T}}(t))^{-1},\ldots,\mathbf{a}_{np}(t)\otimes(\boldsymbol{\sigma}(t)\boldsymbol{\sigma}^{\mathrm{T}}(t))^{-1})^{\mathrm{T}}$, then the exact maximum likelihood estimator of parameters is given by [16]

$$\mathrm{Vec}(\widehat{\mathbf{P}})=-\left(\int_0^T\mathbf{R}(t)\,\mathrm{d}t\right)^{-1}\mathrm{Vec}\left(\int_0^T(\boldsymbol{\sigma}(t)\boldsymbol{\sigma}^{\mathrm{T}}(t))^{-1}\,\mathrm{d}\mathbf{z}_{p-1}(t)\tilde{\mathbf{Y}}^{\mathrm{T}}(t)\right), \tag{23}$$

where $\mathrm{Vec}(\cdot)$ is a column vector valued function listing the columns of the matrix in brackets one below the other and $\otimes$ represents the Kronecker product.

4.2. Parameter estimation for the CARMA model

CARMA(p,q) process

$$\mathbf{X}^{(p)}(t)+\mathbf{A}_1\mathbf{X}^{(p-1)}(t)+\cdots+\mathbf{A}_{p-1}\dot{\mathbf{X}}(t)+\mathbf{A}_p\mathbf{X}(t)=\boldsymbol{\sigma}_0(t)D\mathbf{W}(t)+\cdots+\boldsymbol{\sigma}_q(t)D^{(q+1)}\mathbf{W}(t) \tag{24}$$

can also be written in another state space form, namely, the ancillary variable model. The following is the detailed description of the new form.

Introducing the ancillary variable $\mathbf{s}(t)$ so that

$$\mathbf{s}^{(p)}(t)+\mathbf{A}_1\mathbf{s}^{(p-1)}(t)+\cdots+\mathbf{A}_{p-1}\dot{\mathbf{s}}(t)+\mathbf{A}_p\mathbf{s}(t)=D\mathbf{W}(t),$$

$$\boldsymbol{\sigma}_q(t)\mathbf{s}^{(q)}(t)+\cdots+\boldsymbol{\sigma}_0(t)\mathbf{s}(t)=\mathbf{X}(t),$$

then the state variables are

$$\tilde{\mathbf{y}}_1(t)=\mathbf{s}(t),$$

$$\dot{\tilde{\mathbf{y}}}_1(t)=\tilde{\mathbf{y}}_2(t)=\dot{\mathbf{s}}(t),$$

$$\vdots$$

$$\dot{\tilde{\mathbf{y}}}_p(t)=\mathbf{s}^{(p)}(t)=-\mathbf{A}_p\tilde{\mathbf{y}}_1(t)-\mathbf{A}_{p-1}\tilde{\mathbf{y}}_2(t)-\mathbf{A}_1\tilde{\mathbf{y}}_p(t)+\boldsymbol{\sigma}_0(t)D\mathbf{W}(t).$$

Assume that $\boldsymbol{\sigma}_0(t),\ldots,\boldsymbol{\sigma}_q(t)$ are all continuous functions on the observed interval [0,T], therefore, there exists a sequence $\{t_i\}$ of real numbers with $0=t_0<t_1<\cdots<t_k=T$ which can divide [0,T] into k consecutive subintervals $T_1,\ldots,T_k$, and $\boldsymbol{\sigma}_i(t)$ is approximately equal to a constant matrix on the subinterval T_i (i=1,…,k). Then Eq. (24) can be rewritten into the state-space form on every interval T_i (i=1,…,k):

$$\mathbf{X}(t)=(\boldsymbol{\sigma}_0(t_i),\boldsymbol{\sigma}_1(t_i),\ldots,\boldsymbol{\sigma}_q(t_i),\mathbf{0},\ldots,\mathbf{0})\tilde{\mathbf{Y}}(t),$$

$$\mathrm{d}\tilde{\mathbf{Y}}(t)=\mathbf{A}\tilde{\mathbf{Y}}(t)\,\mathrm{d}t+\mathbf{C}\,\mathrm{d}\mathbf{W}(t),$$

where $\mathbf{C}=(\mathbf{0},\ldots,\mathbf{0},\mathbf{I}_n)^{\mathrm{T}}$.

For the CARMA(2,1) model, we furthermore assume $\boldsymbol{\sigma}_0(t)$ is a constant matrix, then its two state space models are expressed respectively as follows.

(1) The undetermined coefficient model

$$\mathbf{X}(t)=(\mathbf{I}_n,\mathbf{0})\mathbf{Y}(t), \tag{25}$$

$$\mathrm{d}\mathbf{Y}(t)=\mathbf{A}\mathbf{Y}(t)\,\mathrm{d}t+\mathbf{C}(t)\,\mathrm{d}\mathbf{W}(t), \tag{26}$$

where $\mathbf{Y}(t)=(\mathbf{Y}_0^T(t),\mathbf{Y}_1^{\mathrm{T}}(t))^{\mathrm{T}}$ denotes the 2n-dimensional column vector, $\mathbf{Y}_i(t)$ (i=0,1) is the n-dimensional column vector, $\mathbf{C}(t)=(\boldsymbol{\beta}_1^{\mathrm{T}}(t),\boldsymbol{\beta}_2^{\mathrm{T}}(t))^{\mathrm{T}}$ and $\mathbf{A}=\begin{pmatrix}\mathbf{0} & \mathbf{I}_n\\ -\mathbf{A}_2 & -\mathbf{A}_1\end{pmatrix}$, $\boldsymbol{\beta}_1(t)=\boldsymbol{\sigma}_1(t)$, $\boldsymbol{\beta}_2(t)=\boldsymbol{\sigma}_0-\mathbf{A}_1\boldsymbol{\sigma}_1(t)+\dot{\boldsymbol{\sigma}}_1(t)$.

(2) The ancillary variable model: Assume $\boldsymbol{\sigma}_1(t)$ is the piecewise continuous function, the state-space model on every interval T_i (i=1,…,k) is expressed by

$$\mathbf{X}(t)=(\boldsymbol{\sigma}_0,\boldsymbol{\sigma}_1(t_i))\tilde{\mathbf{Y}}(t), \tag{27}$$

$$\mathrm{d}\tilde{\mathbf{Y}}(t)=\mathbf{A}\tilde{\mathbf{Y}}(t)\,\mathrm{d}t+\mathbf{C}\,\mathrm{d}\mathbf{W}(t), \tag{28}$$

where $\mathbf{C}=(\mathbf{0},\mathbf{I}_n)^{\mathrm{T}}$.

4.2.1. Estimation for $\boldsymbol{\sigma}_1(t)$

Let us consider the undetermined coefficient model firstly. When h tends to zero and $\mathbf{A}$ has the form in Section 3, the sub-matrices $\mathbf{H}_{11}$ and $\mathbf{H}_{22}$ of $e^{\mathbf{A}h}$ always approximate to the identity matrices, and $\mathbf{H}_{21}$ approximates to zero matrix, so

$$e^{-\mathbf{A}h} \approx \begin{pmatrix} \mathbf{I} & \mathbf{0} \\ * & \mathbf{H}_{22}^{-1} \end{pmatrix}.$$

Just as in Section 4.1.2, we have

$$E(\mathbf{Y}(t+h)-e^{\mathbf{A}h}\mathbf{Y}(t))(\mathbf{Y}(t+h)-e^{\mathbf{A}h}\mathbf{Y}(t))^{\mathrm{T}} = \begin{pmatrix} \int_0^h \boldsymbol{\beta}_1(t+u)\boldsymbol{\beta}_1^{\mathrm{T}}(t+u)\,\mathrm{d}u & \int_0^h f_1(\boldsymbol{\beta}_2(t))\,\mathrm{d}t \\ \int_0^h f_2(\boldsymbol{\beta}_2(t))\,\mathrm{d}t & \int_0^h f_3(\boldsymbol{\beta}_2(t))\,\mathrm{d}t \end{pmatrix}, \tag{29}$$

where $f_i(\boldsymbol{\beta}_2(t))$ $(i=1,2,3)$ denotes the function with respect to $\boldsymbol{\beta}_2(t)$.

On the interval T_i, Eq. (29) can be estimated by

$$\begin{pmatrix} \boldsymbol{\sigma}_1(t_i)\boldsymbol{\sigma}_1^{\mathrm{T}}(t_i)h & \widehat{\int_0^h f_1(\boldsymbol{\beta}_2(t_i))\,\mathrm{d}t} \\ \int_0^h f_2(\boldsymbol{\beta}_2(t_i))\,\mathrm{d}t & \int_0^h f_3(\boldsymbol{\beta}_2(t_i))\,\mathrm{d}t \end{pmatrix} = \begin{pmatrix} \mathbf{V}_{11} & \mathbf{V}_{12} \\ \mathbf{V}_{21} & \mathbf{V}_{22} \end{pmatrix}.$$

Table 1
Damping matrices of the seven-storey frame structure (kN s/m).

Theoretical values

958	−481	0	0	0	0	0
−481	1127	−646	0	0	0	0
0	−646	1292	−646	0	0	0
0	0	−646	1292	−646	0	0
0	0	0	−646	1200	−554	0
0	0	0	0	−554	1108	−554
0	0	0	0	0	−554	554

Identified results: $\rho_L = 1$

958	−485	9	1	−13	11	−2
−481	1123	−638	2	−14	11	−2
0	−649	1299	−645	−11	9	−2
0	−4	−639	1294	−658	9	−2
14	−24	25	−662	1195	−530	−13
15	−25	25	−16	−560	1133	−567
16	−26	27	−18	−6	−528	541

Identified results: $\rho_L = 2$

962	−457	−46	43	−14	−20	14
−477	1151	−692	43	−14	−20	14
0	−651	1303	−641	−22	30	−17
0	−5	−636	1298	−669	31	−18
16	−28	33	−677	1224	−564	3
17	−30	35	−32	−530	1098	−551
−40	36	−126	167	−97	−491	513

Identified results: $\rho_L = 3$

965	−480	−10	10	2	−14	9
−475	1128	−657	11	2	−14	9
6	−646	1284	−637	1	−12	8
−2	2	−646	1289	−638	−5	2
−2	2	0	−650	1209	−559	2
−2	2	0	−4	−545	1103	−553
−36	97	−112	87	−18	−642	633

Identified results: $\rho_L = 4$

994	−489	59	−100	11	42	−8
−471	1133	−632	6	−39	36	−20
17	−655	1354	−599	75	27	−7
43	−53	−594	1318	−632	−5	−22
38	29	−9	−662	1217	−545	19
−26	24	68	−44	−560	1138	−551
−68	−26	89	−10	−54	−548	558

However, in the above equations, except $\mathbf{V}_{11}=\boldsymbol{\sigma}_1(t_i)\boldsymbol{\sigma}_1^{\mathrm{T}}(t_i)h$, the other equations are all nonlinear functions with respect to the unknown parameters, which means we can get the parameters estimator easily only by solving $\mathbf{V}_{11}/h=\boldsymbol{\sigma}_1(t_i)\boldsymbol{\sigma}_1^{\mathrm{T}}(t_i)$.

4.2.2. Estimation for $\boldsymbol{A}$

After obtaining the estimator of $\boldsymbol{\sigma}_1(t_i)$, we can compute the state vector from the ancillary variable model on every interval T_i, then the structural parameters can be estimated by the undetermined coefficient model just as in Section 4.1.1.

5. Simulations

To demonstrate the effectiveness and accuracy of the system identification methodology presented above, we carry out some numerical simulations in Matlab on a seven-storey shear-building model with the following properties. The mass matrix is **M**=diag(723 714, 686 091, 549 693, 549 693, 549 693, 549 693, 549 693) kg, with diag(·) designating diagonal matrix. The viscous damping and stiffness matrices are shown respectively in the (2)–(8) rows of Tables 1 and 2.

5.1. Simulations by the CAR model

Assume that the random excitation is a continuous time white noise modulated by the uniformly modulated function, then it is variance non-stationary with the variety of the uniformly modulated function. Now we assume the structure is

Table 2
Stiffness matrices of the seven-storey frame structure (10^5 N/m).

Theoretical values						
6729	−3320	0	0	0	0	0
−3320	7309	−3989	0	0	0	0
0	−3989	7978	−3989	0	0	0
0	0	−3989	7978	−3989	0	0
0	0	0	−3989	7651	−3662	0
0	0	0	0	−3662	7324	−3662
0	0	0	0	0	−3662	3662
Identified results: $\rho_L=1$						
6743	−3344	32	−18	−9	15	−6
−3333	7293	−3955	−25	19	−11	2
−1	−3975	7964	−4017	48	−2	−15
−10	5	−3999	7990	−4005	13	−2
12	−16	−7	−3986	7675	−3694	15
12	−17	−10	32	−3685	7337	−3667
3	−26	33	−13	−4	−3663	3665
Identified results: $\rho_L=2$						
6727	−3313	−12	13	−9	1	1
−3322	7316	−4001	13	−9	1	2
−8	−3974	7960	−3984	7	−4	0
−8	16	−4008	7983	−3982	−4	0
0	−3	18	−4021	7674	−3671	2
0	−3	19	−33	−3638	7315	−3660
28	−56	74	−71	54	−3687	3667
Identified results: $\rho_L=3$						
6730	−3322	2	−4	4	0	−1
−3319	7307	−3987	−4	4	0	−1
1	−3991	7980	−3992	3	0	−1
0	−4	−3981	7972	−3986	−3	2
0	−5	8	−3995	7654	−3665	2
0	−5	9	−7	−3659	7321	−3660
28	−61	55	−12	20	−3716	3694
Identified results: $\rho_L=4$						
6729	−3322	2	0	−1	2	−1
−3320	7307	−3986	0	−1	2	−1
0	−3991	7980	−3989	−1	2	−1
0	−2	−3987	7978	−3990	2	−1
−2	2	4	−3997	7657	−3667	3
−2	2	4	−8	−3655	7318	−3659
−2	2	4	−9	7	−3668	3666

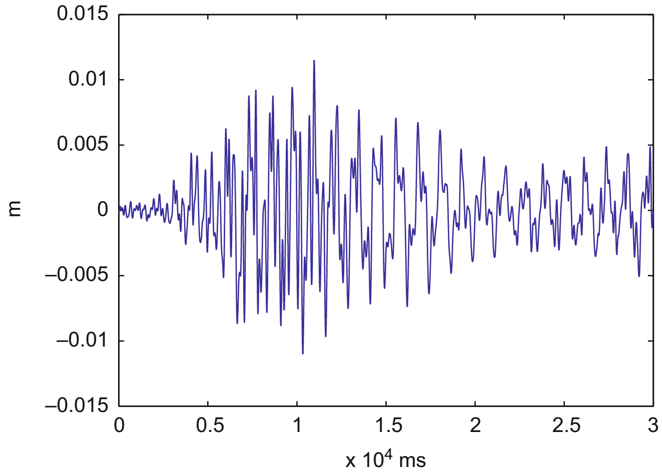

Fig. 1. Displacement response at the 1st floor of the seven-storey frame structure.

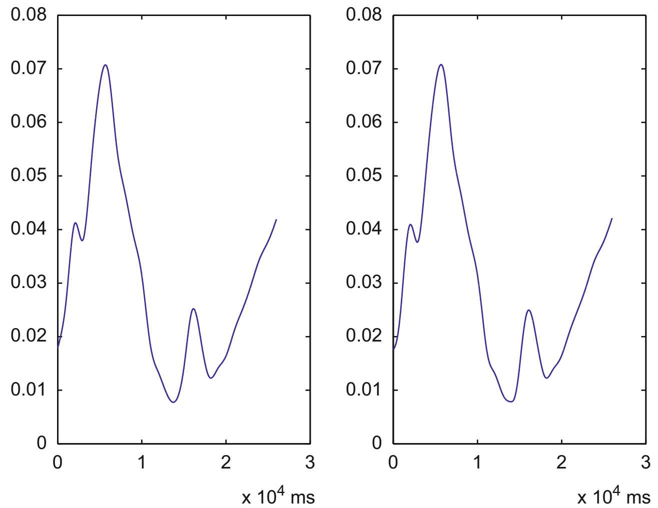

Fig. 2. Modulated functions at the 1st floor of the seven-storey frame structure. The left represents theoretical values and the right represents identified results.

Table 3
Natural frequencies and damping ratios of the seven-storey frame structure.

Mode	Theoretical values		Identified results: $\rho_L = 1$	
	Frequency (Hz)	Damping ratio (%)	Frequency (Hz)	Damping ratio (%)
1	0.8483	0.0040	0.8467	0.0042
2	2.4303	0.0116	2.4287	0.0116
3	3.9407	0.0190	3.9407	0.0189
4	5.2585	0.0249	5.2569	0.0249
5	6.2818	0.0302	6.2818	0.0303
6	7.3100	0.0357	7.3100	0.0356
7	8.1853	0.0410	8.1853	0.0410

excited by the variance non-stationary time-uncorrelated Gaussian random force, then its structural dynamic equation can be described by the CAR(2) model.

In the simulation process, the continuous-time Gaussian white noise is generated by $dW(t)/dt$, where $W(t)$ is a standard Brownian motion. The uniformly modulated function is a continuous function with respect to the time t. Its value determines not only the oscillation level of the random excitation but also the amplitude of the displacement of a system.

In the simulation, the value of the uniformly modulated function is controlled by the allowed maximum displacement of the structure. The selection of the simulation time lies on the estimation of the uniformly modulated function. In this paper we assume that the uniformly modulated function is a piecewise smooth function, the length of each period is set to 1 s. By

Table 4
Natural frequencies and damping rations of the seven-storey frame structure: $\rho_L = 2,3,4$.

Mode	$\rho_L = 2$		$\rho_L = 3$		$\rho_L = 4$	
	Frequency (Hz)	Damping ratio (%)	Frequency (Hz)	Damping ratio (%)	Frequency (Hz)	Damping ratio (%)
1	0.8467	0.0038	0.8483	0.0047	0.8467	0.0067
2	2.4287	0.0120	2.4287	0.0116	2.4303	0.0130
3	3.9407	0.0184	3.9391	0.0195	3.9407	0.0197
4	5.2553	0.0249	5.2585	0.0253	5.2569	0.0266
5	6.2834	0.0300	6.2898	0.0305	6.2755	0.0312
6	7.3052	0.0363	7.3100	0.0365	7.3100	0.0364
7	8.1917	0.0409	8.1869	0.0408	8.1981	0.0403

Table 5
Modal shapes of the seven-storey frame structure.

Theoretical values						
1.0000	1.0000	1.0000	1.0000	1.0000	1.0000	1.0000
1.9650	1.5186	0.6898	−0.3537	−1.3721	−2.5784	−3.7487
2.6723	1.3413	−0.2961	−0.8160	0.3334	3.8121	9.3820
3.2751	0.7331	−1.0317	−0.0504	1.3226	−0.8952	−11.7416
3.7499	−0.1107	−0.8953	0.7911	−0.5301	−2.9964	10.0041
4.1074	−0.9910	0.0776	0.4109	−1.3075	4.2168	−6.0956
4.2901	−1.5246	0.9791	−0.6428	0.9753	−1.9422	2.0475
Identified results: $\rho_L = 1$						
1.0000	1.0000	1.0000	1.0000	1.0000	1.0000	1.0000
1.9632	1.5191	0.6926	−0.3536	−1.3628	−2.4880	−3.6429
2.6698	1.3407	−0.3001	−0.8222	0.3181	3.6684	9.3796
3.2736	0.7319	−1.0431	−0.0400	1.2920	−0.9014	−11.8009
3.7490	−0.1158	−0.9049	0.7998	−0.5093	−2.8394	10.1204
4.1064	−1.0018	0.0763	0.4089	−1.2600	4.0007	−6.2625
4.2898	−1.5388	0.9836	−0.6480	0.9504	−1.8171	2.1423
Identified results: $\rho_L = 2$						
1.0000	1.0000	1.0000	1.0000	1.0000	1.0000	1.0000
1.9652	1.5188	0.6906	−0.3525	−1.3728	−2.5869	−3.8808
2.6731	1.3418	−0.2948	−0.8175	0.3382	3.8022	9.6704
3.2765	0.7334	−1.0319	−0.0521	1.3154	−0.9028	−12.1998
3.7518	−0.1110	−0.8977	0.7928	−0.5428	−3.0247	10.4943
4.1094	−0.9923	0.0766	0.4152	−1.3039	4.2407	−6.3540
4.2916	−1.5267	0.9822	−0.6421	0.9803	−1.9267	2.3636
Identified results: $\rho_L = 3$						
1.0000	1.0000	1.0000	1.0000	1.0000	1.0000	1.0000
1.9648	1.5185	0.6904	−0.3534	−1.3822	−2.5761	−3.7162
2.6717	1.3412	−0.2954	−0.8147	0.3514	3.8085	9.3278
3.2740	0.7331	−1.0318	−0.0486	1.3274	−0.8913	−11.6723
3.7481	−0.1106	−0.8966	0.7894	−0.5552	−2.9913	10.0123
4.1049	−0.9911	0.0758	0.4064	−1.3014	4.2120	−6.1406
4.2865	−1.5250	0.9784	−0.6445	1.0083	−1.9332	2.1992
Identified results: $\rho_L = 4$						
1.0000	1.0000	1.0000	1.0000	1.0000	1.0000	1.0000
1.9650	1.5186	0.6891	−0.3537	−1.3723	−2.5708	−3.7494
2.6723	1.3412	−0.2973	−0.8164	0.3340	3.8062	9.3894
3.2752	0.7329	−1.0329	−0.0509	1.3227	−0.8923	−11.7601
3.7500	−0.1109	−0.8960	0.7910	−0.5308	−2.9868	10.0371
4.1076	−0.9913	0.0789	0.4103	−1.3093	4.1956	−6.0867
4.2904	−1.5248	0.9821	−0.6442	0.9749	−1.9371	2.0666

the spline interpolation, we obtain the estimator of the uniformly modulated function. However, for the spline interpolation method, too much or too little datum will affect the calculation accuracy, so we take the simulation time for about 30 s. The simulated time history of the displacement response at the 1st floor of the seven-storey frame structure in 30 s is shown in Fig. 1, the sampling period is 0.001 s. From Fig. 1, we can see that the non-stationarity is evident in terms of variance.

In order to identify stiffness and damping matrices, we first need to estimate the uniformly modulated functions. The theoretical and identified uniformly modulated functions at the 1st floor are shown in Fig. 2. As observed from Fig. 2, the identified uniformly modulated function hardly differs from the theoretical curve. The maximum relative error in identifying the uniformly modulated function is less than 9 percent.

In simulation process, we also introduce the time history of wind velocity (denoted as ρ_L) in order to consider the spatial correlation of wind load.

The theoretical damping matrix of the building is presented in rows (2)–(8) of Table 1 for comparison. The identified results, when ρ_L varies from 1 to 4, are presented in the rest rows. As one would expect that these identified results are very close to the theoretical values too.

The analogous results are true for the stiffness matrices. Table 2 shows the theoretical values and the identified results.

It is observed from Tables 1 and 2 that these identified results agree well with the theoretical values. For all cases, the maximum error in identifying the stiffness is less than 0.9 percent, whereas the maximum error in identifying the damping is also less than 5 percent.

To gain a further insight into the modal parameters, we carry out the eigenvalue analysis method after obtaining the physical parameters of the building. The theoretical frequencies and damping ratios of the building are presented in columns (2) and (3) of Table 3 for comparison. The identified frequencies and damping ratios for $\rho_L = 1$ are presented in columns (4) and (5). As shown in Table 3, these identified results are very close to the theoretical values. For all cases, the maximum error in identifying the natural frequencies is less than 0.2 percent, whereas the maximum error in identifying the damping ratio is also rather small and is less than 5 percent.

The identified frequencies and damping ratios, when ρ_L varies from 2 to 4, are presented in columns (2)–(7) of Table 4. It is observed from Tables 3 and 4 that these identified results are very close to the theoretical values. Compared with Table 3, when ρ_L varies from 2 to 4, it is gradually decreased in identification efficiency. But for all cases, the maximum

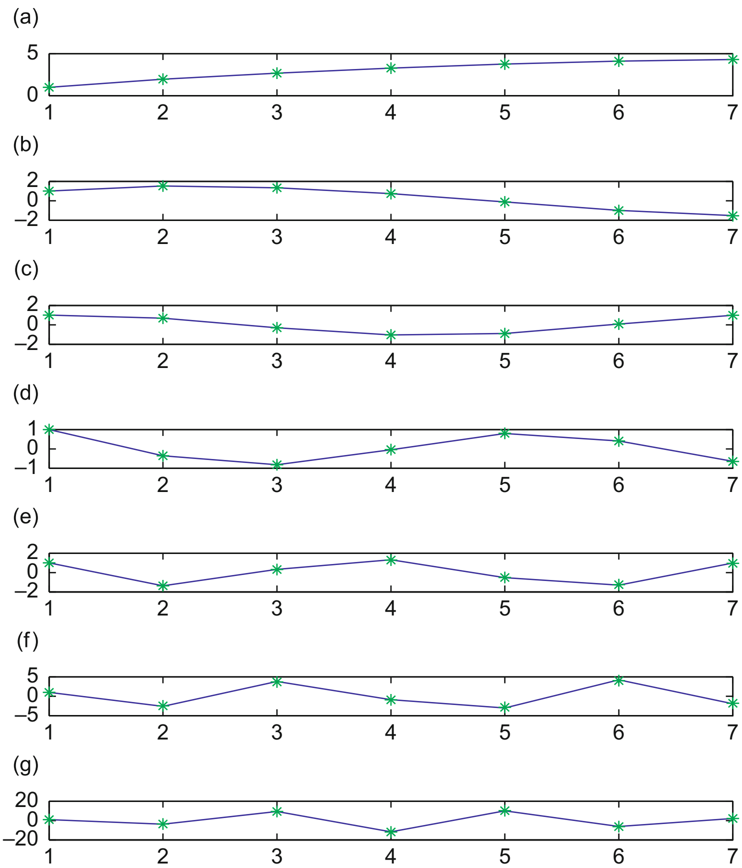

Fig. 3. Modal shapes of seven-storey frame structure. Solid line represents the theoretical values and ∗ represents the identified results. It denotes, from (a) to (g) respectively, the 1–7th modal shapes.

Table 6
Damping matrices of the seven-storey frame structure corrupted by noise (kN s/m).

SNR=85						
1238	−580	80	−102	−2	−57	43
−585	1492	−823	−42	28	−14	−8
−19	−751	1600	−763	43	28	−75
4	34	−694	1444	−642	−9	−20
−28	−5	−58	−679	1413	−643	12
8	−29	32	0	−696	1364	−658
14	29	−112	−58	71	−672	778
SNR=90						
1062	−504	24	−20	−29	58	−13
−530	1274	−769	60	−66	23	−12
6	−646	1383	−709	−51	72	−24
−54	36	−681	1404	−676	16	−28
−29	39	−29	−692	1385	−700	23
31	−52	52	−53	−579	1307	−619
21	4	−57	−15	22	−647	685
SNR=100						
1022	−534	15	40	−19	0	4
−441	1220	−761	36	94	−97	3
−7	−664	1350	−684	10	45	−42
−9	0	−610	1231	−620	21	6
−33	50	20	−670	1240	−580	−20
−39	8	−44	−12	−507	1149	−586
−17	−69	77	−52	15	−568	598
SNR=110						
1032	−477	−8	21	−90	26	19
−447	1133	−610	−49	−21	−13	44
27	−633	1281	−647	−5	−43	34
−37	20	−688	1388	−639	4	−26
−36	40	−24	−629	1204	−569	−16
66	−92	12	29	−571	1161	−564
−29	90	−57	48	−53	−565	612
SNR=120						
1032	−472	−19	−47	73	−98	55
−501	1188	−650	−64	5	−29	19
−34	−674	1355	−651	65	−49	−5
−44	44	−636	1244	−559	−54	12
−36	11	−52	−609	1249	−566	7
14	7	−40	52	−649	1189	−552
10	27	−101	22	−18	−551	632

error in identifying the natural frequencies is less than 0.2 percent, whereas the maximum error in identifying the damping ratio is also rather small. However, the larger the time history of the wind velocity becomes, the larger the maximum identified error is.

The rows of (2)–(8) in Table 5 present the theoretical modal shapes for comparison. The identified results are presented in the remaining rows of Table 5. The identified results agree well with the theoretical values. We can also reach the conclusion from Fig. 3.

In order to check the robustness of this method, Gaussian random disturbance forces are added to the response datum. The simulation results show that when the signal-noise-ratio (SNR) is higher than 85 dB, the approach is robust. The identified damping and stiffness matrices, when SNR varies from 85 to 120 dB, are presented in Tables 6 and 7. It is observed from Tables 6 and 7 that with the increase of SNR, these identified results are more and more close to the theoretical values, and eventually stabilize at the theoretical values. The result can be concluded from Fig. 4, which show the 2nd modal shape when SNR varies from 30 to 150 dB.

5.2. Simulation by the CARMA model

Assuming the structure is excited by the covariance non-stationary Gaussian random force, then its structural dynamic equation can be described by the CARMA(2,1) model. The theoretical and identified uniformly modulated functions are

Table 7
Stiffness matrices of the seven-storey frame structure corrupted by noise (10^5 N/m).

SNR=85						
6737	−3314	−2	−29	20	−18	22
−3312	7298	−3957	−28	−20	26	−6
−4	−3988	7972	−3984	−1	11	−12
2	7	−4011	7984	−3983	11	−10
10	−10	10	−4002	7658	−3658	−2
5	4	−28	29	−3666	7304	−3647
14	−44	66	−53	37	−3672	3657
SNR=90						
6751	−3332	1	−2	10	2	−9
−3328	7329	−3997	−14	22	−26	13
12	−4003	7986	−3985	−14	−10	15
15	12	−4036	8018	−4002	−2	6
−5	0	8	−4001	7658	−3652	−8
14	−23	3	22	−3686	7330	−3660
5	−11	13	−12	−8	−3634	3646
SNR=100						
6715	−3295	−25	9	8	−13	7
−3324	7313	−4006	34	−22	−15	18
17	−4002	7989	−3991	−8	−5	8
−23	18	−3999	7996	−4010	13	−5
13	−13	8	−4001	7678	−3691	11
−8	10	−8	14	−3681	7340	−3669
14	−16	35	−48	36	−3684	3669
SNR=110						
6736	−3334	44	−40	−1	−5	12
−3313	7288	−3957	−12	−10	5	0
−7	−3983	7975	−4000	14	13	−17
16	−1	−4008	7978	−3976	−2	0
2	−6	23	−4013	7656	−3669	10
20	−15	6	11	−3686	7324	−3651
2	−7	0	16	−31	−3618	3637
SNR=120						
6720	−3299	−17	6	−11	−8	17
−3328	7312	−3976	−11	−18	23	−9
−5	−3983	7967	−3984	0	19	−19
18	−14	−3996	7994	−3999	8	−4
15	−21	23	−4015	7674	−3674	4
−18	27	−38	29	−3674	7311	−3647
23	−44	55	−42	36	−3685	3667

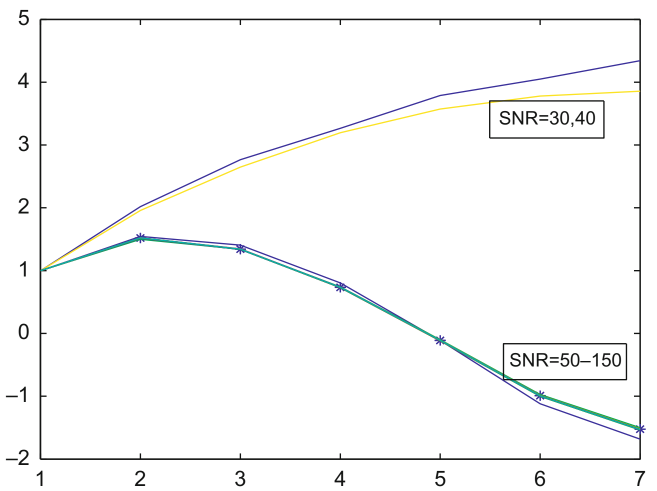

Fig. 4. The 2nd modal shape of seven-storey frame structure corrupted by noise. SNR varies from 30 to 150 dB. '*' represents the theoretical values.

shown in Fig. 5. As observed from Fig. 5, the identified uniformly modulated function hardly differ from the theoretical curves, but the identified errors become larger compared with the identified results from the CAR(2) model.

The identified damping matrix by the CARMA model is presented in Table 8. It is observed from Tables 1 and 8 that the identified results are very close to the theoretical values. However, we also see that the identified precision declines compared with that of the CAR model. The analogous results are true for the stiffness matrices. The identified results are presented in Table 9.

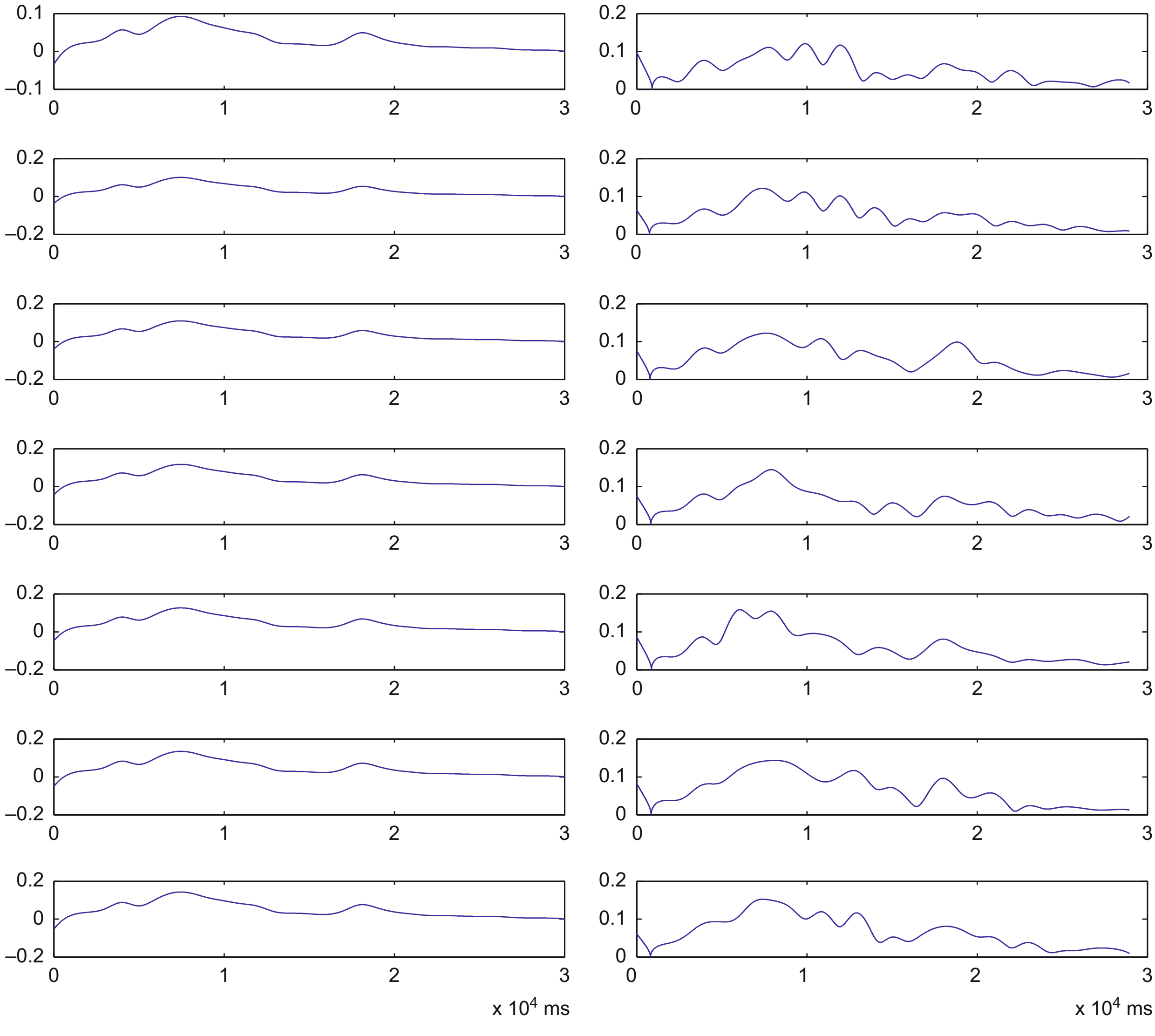

Fig. 5. Modulated functions of seven-storey frame structure. The left represents the theoretical values and the right represents identified results.

Table 8
Identified damping matrix of the seven-storey frame structure by the CARMA model (kN s/m).

1019	−523	54	16	−118	76	−9
−442	1207	−601	−44	−50	−42	50
12	−580	1265	−646	39	−24	9
−38	6	−756	1494	−697	−10	10
−111	72	−94	−552	1156	−572	12
137	−72	11	−63	−612	1236	−548
3	60	−85	81	−149	−469	670

Table 9
Identified stiffness matrix of the seven-storey frame structure by the CARMA model (10^5 N/m).

6721	−3327	74	−90	28	6	−2
−3299	7266	−3937	−19	−27	40	−22
−1	−3952	7896	−3953	38	−18	−8
38	−33	−3929	7856	−3905	−39	22
17	2	8	−3962	7576	−3637	8
−7	25	−22	−18	−3583	7199	−3597
−30	20	−37	50	−42	−3591	3609

Table 10
Natural frequencies and damping ratios of the seven-storey frame structure by the CARMA model.

Mode	Theoretical values		Identified results	
	Frequency (Hz)	Damping ratio (%)	Frequency (Hz)	Damping ratio (%)
1	0.8483	0.0040	0.8372	0.0116
2	2.4303	0.0116	2.4287	0.0165
3	3.9407	0.0190	3.9232	0.0245
4	5.2585	0.0249	5.2362	0.0253
5	6.2818	0.0302	6.2627	0.0316
6	7.3100	0.0357	7.2559	0.0384
7	8.1853	0.0410	8.1344	0.0417

The identified frequencies and damping ratios are presented in columns (4) and (5) of Table 10. It is observed that these identified results are very close to the theoretical values. For all cases, the maximum error in identifying the natural frequencies is rather small, whereas the maximum error in identifying the damping ratio is relatively bigger, especially for the low-frequency situations.

6. Conclusion

A new time-domain CARMA method using response-only data is proposed in this paper. The system parameters include the damping parameters as well as the stiffness parameters of a structure. The proposed method is able to estimate the stiffness and damping properties directly.

Although the CARMA model has been widely used in the traditional modal identification procedures, most of them need to transform the continuous model into a discrete one and then identify modal parameters, which can lead to a low computing efficiency. Our method overcomes the deficiency to a certain extent. And the new identification method is robust when SNR is higher than 85 dB.

Although the method has the advantages mentioned above, many deficiencies can be found. The inevitable deficiency is that the method can identify parameters efficiently only when the random excitation is a Gaussian process, but in practical applications most of the random excitations are not Gaussian. Therefore, further study is still needed in the future.

References

[1] J. Li, J. Chen, Study on identification of structural dynamic parameters with unknown input information, *Chinese Journal of Computational Mechanics* 16 (1) (1999) 23–32.
[2] J. Chen, J.Y. Wang, G. Lin, A structural parameter identification method without input information, *Engineering Mechanics* 23 (1) (2006) 6–11.
[3] J.S. Kang, S.-K. Park, S. Shin, H.S. Lee, Structural system identification in time domain using measured acceleration, *Journal of Sound and Vibration* 288 (2005) 215–234.
[4] J.S. Sakellariou, S.D. Fassois, Stochastic output error vibration-based damage detection and assessment in structures under earthquake, *Journal of Sound and Vibration* 297 (2006) 1048–1067.
[5] K. Liu, Extension of modal analysis to linear time-varying systems, *Journal of Sound and Vibration* 226 (1) (1999) 149–167.
[6] A.G. Poulimenos, S.D. Fassois, Parametric time-domain methods for non-stationary random vibration modelling and analysis: a critical survey and comparison, *Mechanical Systems and Signal Processing* 20 (4) (2006) 763–816.
[7] M. Jachan, G. Matz, F. Hlawatsch, Time–frequency ARMA models and parameter estimators for underspread non-stationary random processes, *IEEE Transactions on Signal Processing* 55 (9) (2007) 4366–4381.
[8] T.M. Toolan, D.W. Tufts, Detection and estimation in non-stationary environments, *Conference Record of the Thirty-Seventh Asilomar Conference on Signals*, *Systems and Computers*, Vol. 1, 2003, pp. 797–801.
[9] P. Mohanty, D.J. Rixen, A modified Ibrahim time domain algorithm for operational modal analysis including harmonic excitation, *Journal of Sound and Vibration* 275 (1–2) (2004) 375–390.
[10] H. Tsai, K.S. Chan, Maximum likelihood estimation of linear continuous time long memory processes with discrete time data, *Journal of Royal Statistical Society Series B* 67 (5) (2005) 703–716.
[11] G.F. Franklin, J.D. Powell, E.-N. Abbas, *Feedback Control of Dynamic Systems*, Higher Education Press, Beijing, 2003.
[12] L. Karatzas, S.E. Shreve, *Brownian Motion and Stochastic Calculus*, Springer, New York, 2000.

[13] C.M. Harris, C.E. Crede, *Shock and Vibration Handbook*, McGraw-Hill Book Company, New York, 1976.
[14] P. Brockwell, R.A. Davis, Y. Yu, Continuous-time Gaussian autoregression, *Statistica Sinica* 17 (1) (2007) 63–80.
[15] D.W. Stroock, S.R.S. Varadhan, *Multidimensional Diffusion Processes*, Springer-Verlag, Berlin, 1979.
[16] X.L. Du, F.Q. Wang, New modal identification method under the non-stationary Gaussian ambient excitation, *Applied Mathematics and Mechanics* 30 (10) (2009) 1295–1304.